

Automatic Detection of Heart Diseases Based on ECG Signal Analysis

Louis Delarue, Pierre-Arnaud Drouard, Pierre Hourdé,
Jean Joulia, Victorien Renault, and Rafal Kotas

Abstract—The authors provide overview of techniques used in ECG signal analysis and present their implementation in order to detect heart diseases (arrhythmias). This paper presents different means to study the ECG signals to develop automatic detection of heart diseases based on artificial intelligence.

Index Terms—ECG, QRS complex, Pan-Tompkins algorithm, arrhythmia, HRV, HRT

I. INTRODUCTION

It is known that the number of heart diseases is increasing since several years: 17,7 million people die every year from cardiovascular diseases. That represents 31% of all global deaths in the world [1]. The Electrocardiogram (ECG) signal analysis offers the possibility to detect diseases using different parameters. ECG is a simple and non-invasive procedure: electrodes are placed on the patient and connected to a monitor, which measure electrical activity of the heart (Fig. 1).

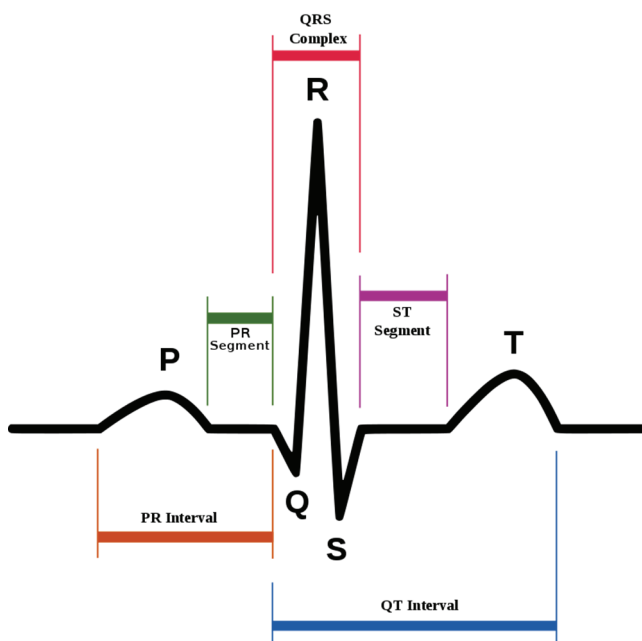


Fig. 1. Typical ECG waveform.

L. Delarue, P.-A. Drouard, P. Hourdé, J. Joulia and V. Renault are with the ISEN Lille Engineering School, 41 boulevard Vauban, 59046 Lille Cedex, France.

R. Kotas is with the Department of Microelectronics and Computer Science, Lodz University of Technology, ul. Wolczanska 221/223, 90-924 Lodz, Poland (e-mail: email: rkotas@dmcs.pl).

PTB and QT Physio Net databases are used for this study. PTB database (PTBDB) [2] contains 549 records from 290 subjects (aged 17 to 87, mean 57.2; 209 men, mean age 55.5, and 81 women, mean age 61.6; ages were not recorded for 1 female and 14 male subjects). Each record includes 15 simultaneously measured signals: the 12 leads (i, ii, iii, avr, avl, avf, v1, v2, v3, v4, v5, v6) together with the 3 Frank lead ECGs (vx, vy, vz). Each signal is digitized at frequency of 1000 Hz, with 16 bits resolution over a range of ± 16.384 mV.

9 pathologies identified in this database are presented in Table I. The clinical summary is not available for 22 out of 290 patients.

TABLE I
THE DIAGNOSTIC CLASSES OF THE REMAINING 268 SUBJECTS

| Diagnostic class | Number of subjects |
|------------------------------|--------------------|
| Myocardial infarction | 148 |
| Cardiomyopathy/Heart failure | 18 |
| Bundle branch block | 15 |
| Dysrhythmia | 14 |
| Myocardial hypertrophy | 7 |
| Valvular heart disease | 6 |
| Myocarditis | 4 |
| Miscellaneous | 4 |
| Healthy controls | 52 |

QT database (QTDB) [2] contains 105 records that come from different databases. Table II shows the distribution of the 105 records according to their original database.

TABLE II
DISTRIBUTION OF THE 105 RECORDS ACCORDING TO THE ORIGINAL DATABASE

| Original database | Diagnostic | Number of subjects |
|-------------------|------------|--------------------|
| MIT-BIH | Arrhythmia | 15 |
| MIT-BIH | ST DB | 6 |
| MIT-BIH | Sup. Vent. | 13 |
| MIT-BIH | Long Term | 4 |
| ESC | STT | 33 |
| MIT-BIH | NSR DB | 10 |
| Sudden | Death | 24 |

This article is divided into three main sections, first of which deals with the methods used to analyse the ECG signals and detect the heart diseases. The second section presents obtained results, while third is a discussion about the results.

II. METHODS

A. ECG signal segmentation algorithms

Segmentation of ECG signal is divided into following stages.

1) QRS waves detection

The diagram shown in Fig. 2 presents the following steps of implemented algorithm. The first part corresponds to the signal pre-processing. The second one is based on the Pan-Tompkins algorithm. [3]

All the units for the temporal representation of the signal are second [s] in x-axis and millivolt [mV] in y-axis. For the frequential representation, the units are frequency [Hz] in x-axis and millivolt [mV] in y-axis.

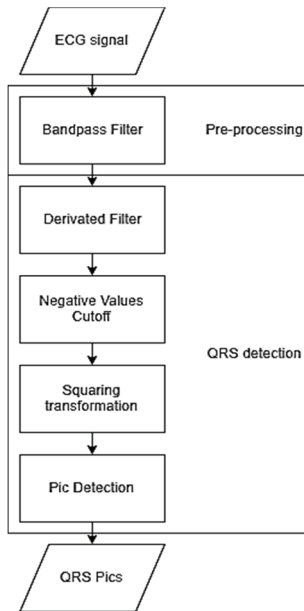


Fig. 2. QRS detection algorithm diagram.

Plots presented in Fig. 3, Fig. 4 and Fig. 5 show two important features:

- the signal contains noise in high frequencies because of the power source itself, but also due to the muscles contractions.
- the signal has a general tendency to go up or down due to a component in low frequency.

It is known that the QRS complex and PT waves have a maximal energy below 40 Hz [4]. The algorithm applies a digital bandpass filter between 1 and 40 Hz to avoid to perturbate P and T and use the same filtered signal for QRS and PT detection.

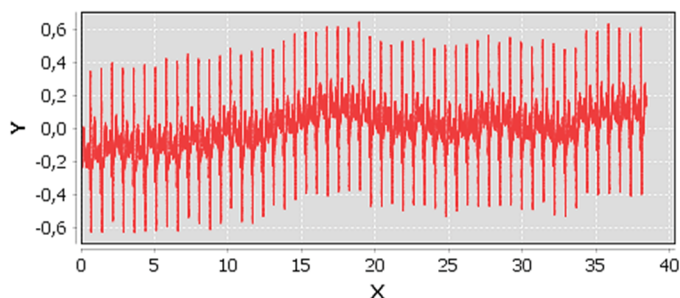


Fig. 3. Original ECG signal of the patient 001.

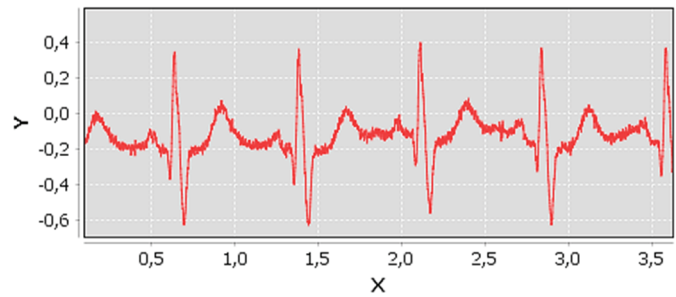


Fig. 4. Original ECG signal of the patient 001 (zoom).

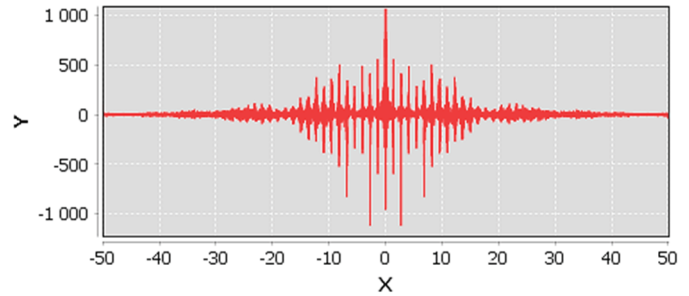


Fig. 5. FFT of the original signal of the patient 001.

a) Signal pre-processing

The Butterworth seems to be the most performant digital filter for this case of signal. This filter permits to have a gain as constant as possible between the bandpass. Fig. 6, Fig. 7 and Fig. 8 show the exemplary result of the filtering process.

Nevertheless, for some signals (even up to 20%), the deformation could be important due to the fact that filters can be the cause of an amplitude's decrease for the R signal.

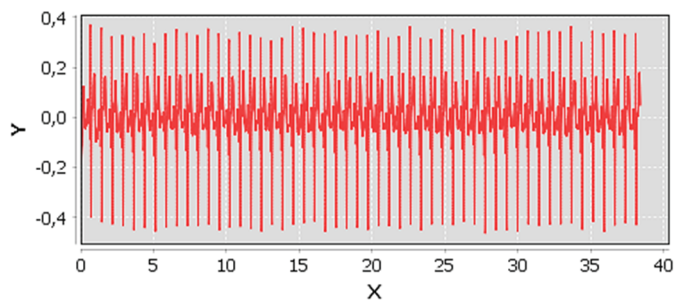


Fig. 6. Filtered signal with bandpass filter.

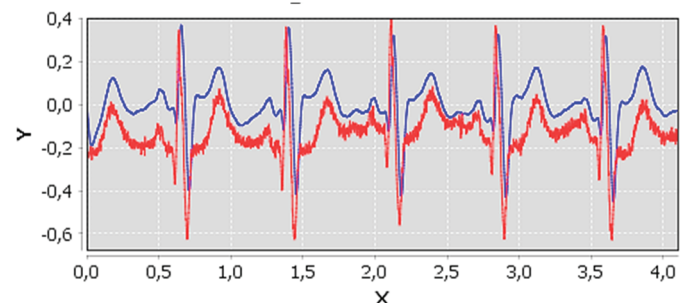


Fig. 7. Comparison of initial signal (red) and filtered signal (blue).

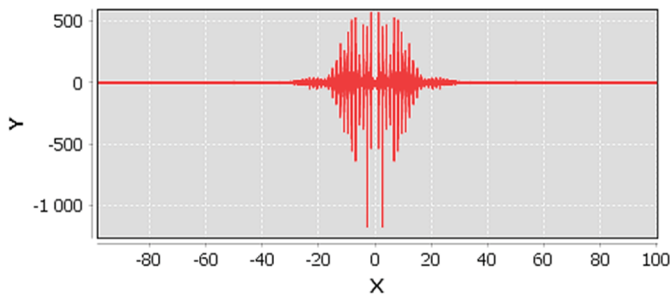


Fig. 8. FFT of the filtered signal.

b) QRS complex detection

The first step is to determine the signal derivative (Fig. 9). The QRS complex is short, usually between 0.02 - 0.2 second. Consequently, the derivative of the signal presents large maximum values, which are necessary for the detection. The derivative filter is sensitive to the noises, that is why the noises must be removed before.

The algorithm uses the following filter:

$$H = \frac{Y}{X} = 1 + 2z^{-1} + 2z^{-2} - z^{-4} \tag{1}$$

$$Y[n] = X[n] + 2X[n - 1] - 2X[n - 3] - X[n - 4] \tag{2}$$

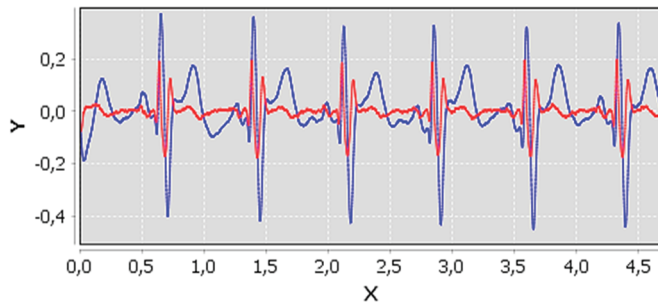


Fig. 9. Signal after applying derivative filter (red) and original signal (blue).

The second step is the squaring transformation, which allows to increase the contrast of the derivation. It allows to eliminate negative values and assures the symmetry of the detection between R and QS signals as it is shown in Figure 10.

$$Y[t] = X[t]^2 \tag{3}$$

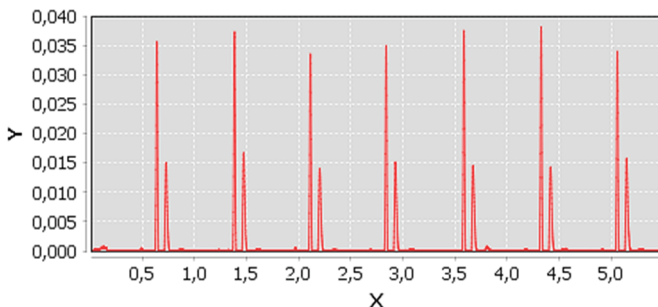


Fig. 10. Signal after applying squaring function and negative values cut-off.

The third step is the peaks detection. It is achieved thanks to a threshold detection. The algorithm checks all local maximum values to calculate an average. After that, it detects all peaks at 30% of the maximum amplitude, which corresponds to the R peaks. When the R peaks are found, the algorithm searches the two minima around the R wave to locate Q and S waves. Exemplary peaks detection results are shown in Figure 11.

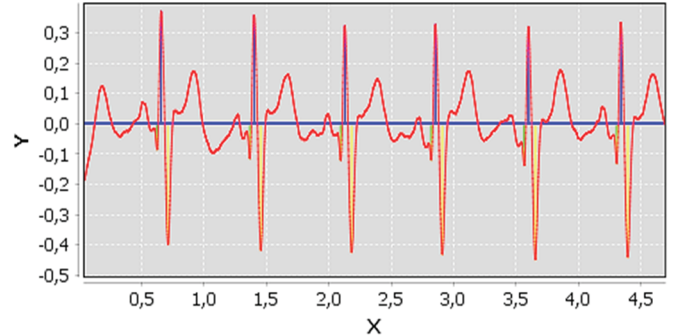


Fig. 11. Exemplary results of QRS detection.

2) P & T waves detection

a) Signal pre-processing

The second part of the ECG signal analysis is the P and T waves detection. To achieve this goal authors used QRS complex and probabilistic approach presented in Figure 12 [5]. The use of a second-order Butterworth filter 0.5 Hz to 10 Hz on the original signal allows for noise removal and keeping the possible P and T waves because they are composed of low

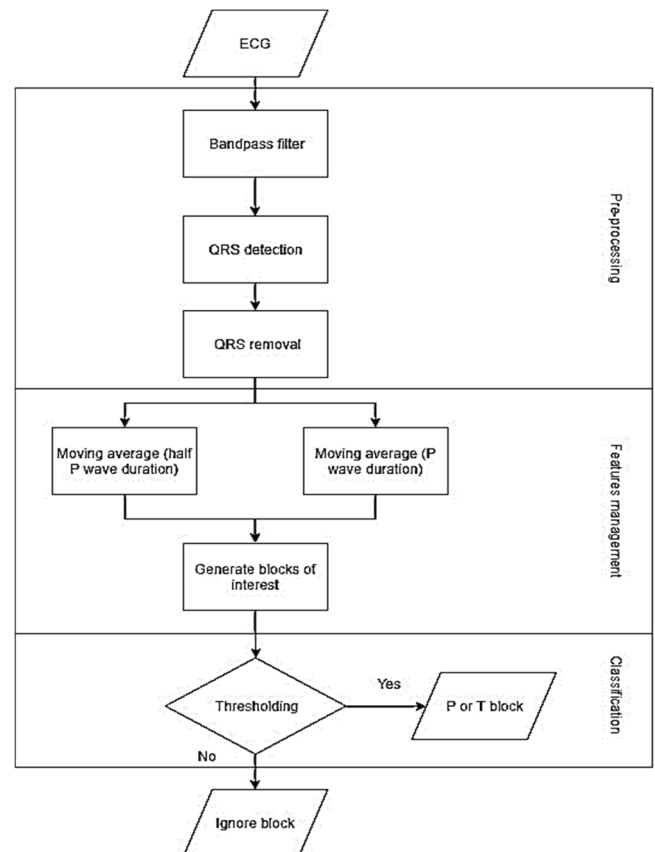


Fig. 12. P & T waves detection algorithm diagram [5].

frequencies. It is necessary to filter the signal once, revert it then apply the same filter for the second time. It eliminates the phase shift effect. After filtering the QRS complex of the resultant signal is removed. Following steps are presented in Figures 13, 14 and 15.

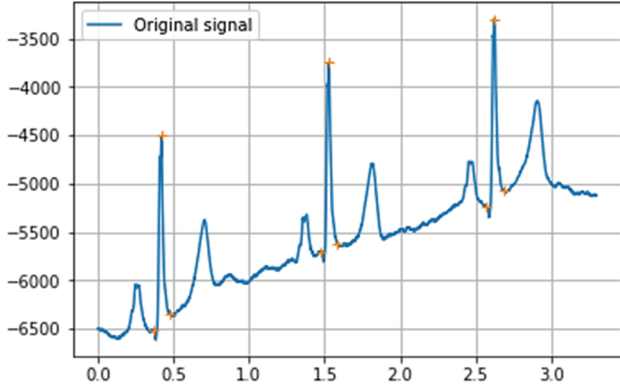


Fig. 13. Original signal with QRS complex already classified (case of an amplified T wave).

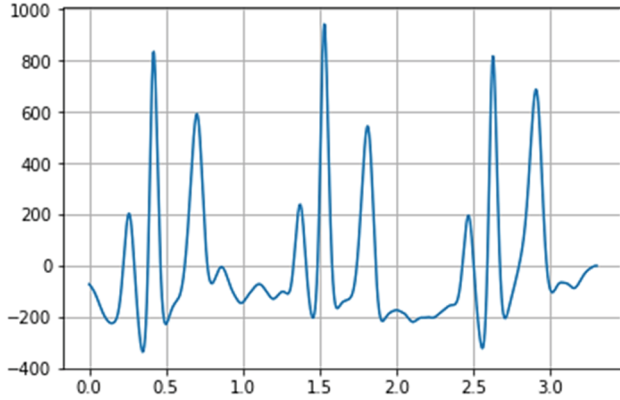


Fig. 14. Filtered signal with Butterworth filter 0.5 Hz – 10 Hz.

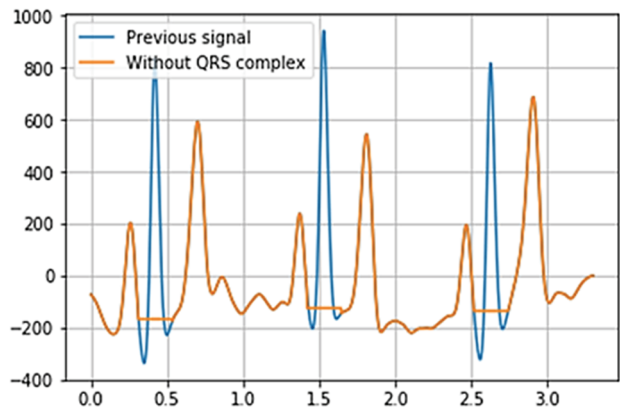


Fig. 15. QRS complex removing.

It is necessary to identify the possible blocks where the algorithm could find the P and T waves. It uses two moving averages of our signal with different widths. The limit of the P wave duration for a healthy adult is 110 ms at heart rate of 60 beats per minute [6]. This information is sufficient to define width of the windows.

$$W_1 = 55\text{ms} * f_s \quad (4)$$

$$W_2 = 110\text{ms} * f_s \quad (5)$$

W_1 equals to the first moving average filter (MA_{peak}) and W_2 equals to the second moving average filter (MA_{wave}) with f_s the frequency sampling. Figure 16 illustrates the following process. If the MA_{peak} line is over the MA_{wave} line, it should be marked as possible blocks.

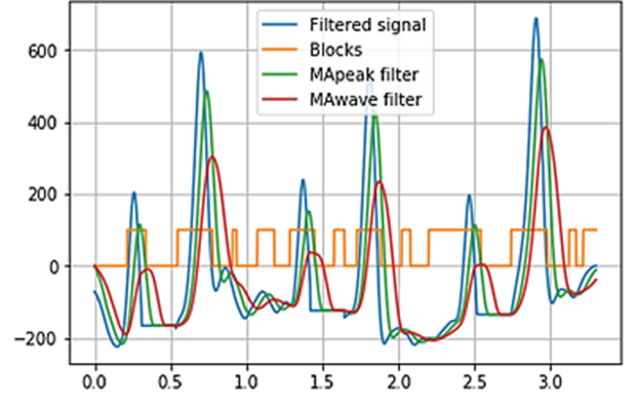


Fig. 16. P and T possible blocks identification.

b) Thresholding

Once all blocks are found, the next step is to identify, which of them could be classified as P or T wave.

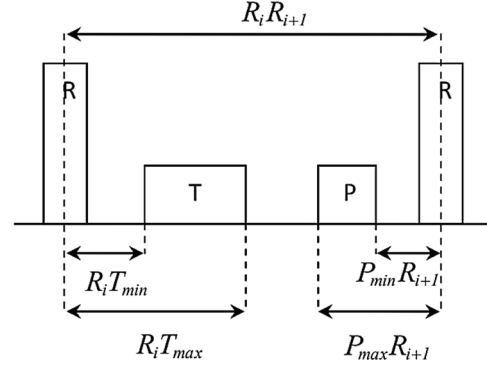


Fig. 17. Locations of P and T wave areas between two R peaks [5].

The search for T waves locations are calculated as:

$$R_i T_{min} = D_{min} R_i R_{i+1} \quad (6)$$

$$R_i T_{max} = D_{max} R_i R_{i+1} \quad (7)$$

$R_i T_{min}$ represents the minimum range between the T wave and the first R peak, $R_i T_{max}$ is the maximum range between the T wave and the same R peak. $R_i R_{i+1}$ represents the interval between the two R peaks (R_i and R_{i+1}) - Figure 17. According to [7], the value of D_{min} and D_{max} are 170 ms and 800 ms.

As presented by the Figure 18, for a detected block called b with b_j and b_{j+1} as its starting and ending point, the following condition must be considered in pseudo-code.

If $((R_i + R_i T_{min} < b_j)$ and $(b_{j+1} < R_i + R_i T_{max}))$

Then b is probably a T wave block

Else b is ignored

For all selected blocks, the best is the nearest one of the first R peak.

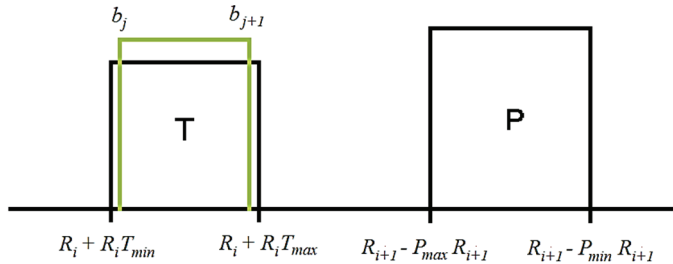


Fig. 18. Example of a valid T block (green).

Similarly, it is the same process as the previous one for P waves. The search for P waves locations are calculated as:

$$P_{min}R_{i+1} = D_{min} R_i R_{i+1} \quad (7)$$

$$P_{max}R_{i+1} = D_{max} R_i R_{i+1} \quad (8)$$

$P_{min}R_{i+1}$ represents the minimum range between the T wave and the second R peak, $P_{max}R_{i+1}$ is the maximum range between the T wave and the same R peak. Once again, $R_i R_{i+1}$ represents the interval between the two R peaks (R_i and R_{i+1}). According to [7], the value of D_{min} and D_{max} are respectively 55 ms and 470 ms. To classify the potential P waves, the same condition must be considered in pseudo-code as with T waves.

If $((R_{i+1} - P_{max}R_{i+1} < b_j)$ and $(b_{j+1} < R_{i+1} - P_{min}R_{i+1}))$

Then b is probably a P wave block

Else b is ignored

For all selected blocks, the best is the nearest one of the second R peak. Figure 19 presents obtained results of P and T waves detection.

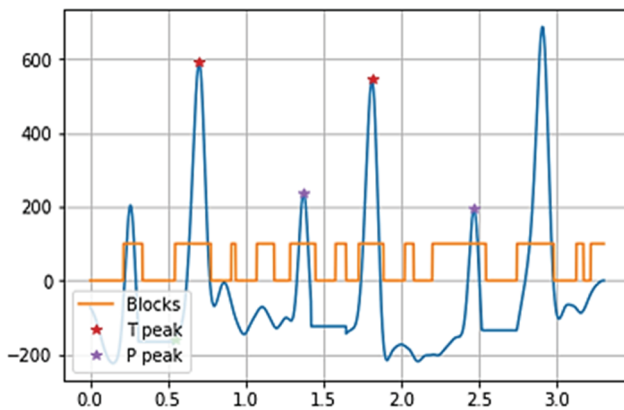


Fig. 19. P and T peaks classification.

B. ECG parameters

Previous ECG signals analysis offers the possibility to detect P-QRS-T waves. The next step is to calculate ECG parameters [8].

1) Heart Rate Turbulence (HRT)

The HRT analysis is used to evaluate the risks of sudden cardiac death in patients with a history of myocardial infarction.

2) Heart Rate Variability (HRV)

This parameter is important to predict the mortality of several diseases.

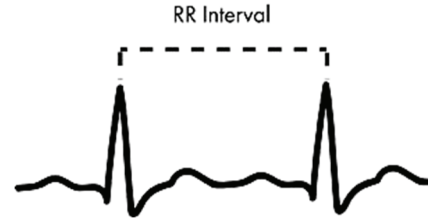


Fig. 20. RR interval on an ECG signal.

In the case where RR interval (shown in Fig.20) is «normal», NN interval designation is preferred. To calculate HRV, several methods can be used: RMSSD (Root Mean Square of Successive Differences), SDNN (Standard Deviation of all NN intervals), SDANN (Standard Deviation of the 5 minute Average NN intervals) method in time domain.

One of the graphic method for HRV presentation is a Poincaré plot. The value of the first RR interval is plotted with the second RR interval. The second RR interval is plotted with the third RR interval and so on. If all the points are closed, the patient has a limited HRV (right picture) whereas on the left the HRV is high. Both SD1 and SD2 are axes of an imaginary ellipse presented in Figure 21. SD1 measures the dispersion of points across the identity line, and SD2 measures the dispersion of points along the identity line.

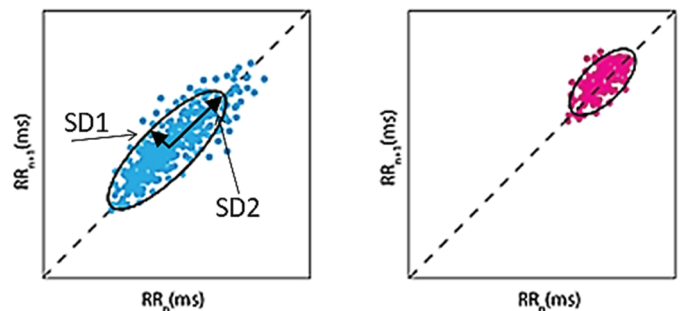


Fig. 21. Representation of Poincaré plot.

SDNN is the simplest method to calculate HRV. It is equivalent to calculate the square root of variance. For higher precision more than 18 hours of ECG recording is required. A similar solution is to apply SDANN method. This analysis is done by taking the average of the RR intervals on several periods of 5 min.

3) Acceleration Capacity/Deceleration Capacity (AC/DC)

Deceleration capacity of heart rate is a predictor of mortality (after myocardial infarction). To detect the AC/DC, 5 steps [9] are necessary:

1. Definition of anchors:
 - For the decelerate capacity, the heartbeat intervals, which are longer than the preceding interval are considered as anchors.
 - For the accelerate capacity, the heartbeat intervals, which are shorter than the preceding interval are identified as anchors.
2. Definition of segments - Around the anchors, segments of the same size must be chosen.
3. Phase rectification - The segments are aligned at the anchors.
4. Signal averaging.
5. Quantification of DC or AC.

All these parameters are useful to detect diseases. Thereafter, all of them are used to automatically diagnose the different diseases.

C. Arrhythmia detection by deep learning

1) Training set

For detection of arrhythmias, MIT-BIH [10] and incart [11] databases are used. MIT-BIH database contains 48 half-hour recordings of two-channel ambulatory ECG recordings. The recordings were digitized at 360 samples per second per channel with 11-bit resolution over a 10mV range. Two or more cardiologists independently annotated each record.

The second database consists of 75 annotated recordings extracted from 32 Holter records. Each record is 30 minutes long registered with the use of 12 standard leads, each sampled at 257 Hz, with gains varying from 250 to 1100 analog-to-digital converter units per millivolt. The reference annotation files contain over 175,000 beat annotations.

2) Pre-processing

All ECG signals from those two databases were reshaped to obtain records with a format of 2 channels and 300 samples (300 samples for the lead II and 300 samples for the lead V5). Each record was saved in a file HDF5 and annotated with one of the five classes (normal beat, Supraventricular ectopic beat, Ventricular ectopic beat, Fusion beat or Unknown beat). Unfortunately this database is not balanced, 80% of the database represent normal heart beat. Therefore the model was not trained with the entire database in order to avoid overfitting.

3) Model

In order to detect these diseases, two models were trained. The first model (configuration shown in Fig. 22) was a classic convolutional neural network model (CNN) build of 8 layers. The advantage of this type of model is the rapidity for training and prediction.

| Layer (type) | Output Shape | Param # |
|-------------------------------|----------------|---------|
| conv1d_41 (Conv1D) | (None, 2, 64) | 19264 |
| conv1d_42 (Conv1D) | (None, 2, 64) | 4160 |
| max_pooling1d_11 (MaxPooling) | (None, 1, 64) | 0 |
| conv1d_43 (Conv1D) | (None, 1, 128) | 8320 |
| conv1d_44 (Conv1D) | (None, 1, 128) | 16512 |
| global_average_pooling1d_11 | (None, 128) | 0 |
| dropout_11 (Dropout) | (None, 128) | 0 |
| dense_19 (Dense) | (None, 5) | 645 |
| Total params: 48,901 | | |
| Trainable params: 48,901 | | |
| Non-trainable params: 0 | | |

Fig. 22. CNN model.

The second model was a LSTM (long short-terms memory) network (configuration shown on Fig. 23). Its layers was also trained on the same dataset to compare the results. The difference between classic convolutional layers and LSTM layers is that LSTM layers allow information to persist and be used for the next prediction.

| Layer (type) | Output Shape | Param # |
|-----------------------------|----------------|---------|
| lstm_1 (LSTM) | (None, 2, 512) | 1665024 |
| lstm_2 (LSTM) | (None, 2, 256) | 787456 |
| lstm_3 (LSTM) | (None, 2, 128) | 197120 |
| lstm_4 (LSTM) | (None, 2, 64) | 49408 |
| lstm_5 (LSTM) | (None, 32) | 12416 |
| dense_1 (Dense) | (None, 5) | 165 |
| Total params: 2,711,589 | | |
| Trainable params: 2,711,589 | | |
| Non-trainable params: 0 | | |

Fig. 23. LSTM model.

III. RESULTS

A. P-QRS-T waves detection

Implemented algorithms were tested and verified on ECG recordings of 50 patients. The results show that 95% of the QRS complexes and 80% of P and T waves were detected correctly. This method is not applicable for 3% of the patients.

With those results it is possible to calculate all the parameters that are needed for a disease detection.

Figures 25 shows exemplary results of P-QRS-T waves detection and Figure 24 shows P-QRS-T peaks selection.

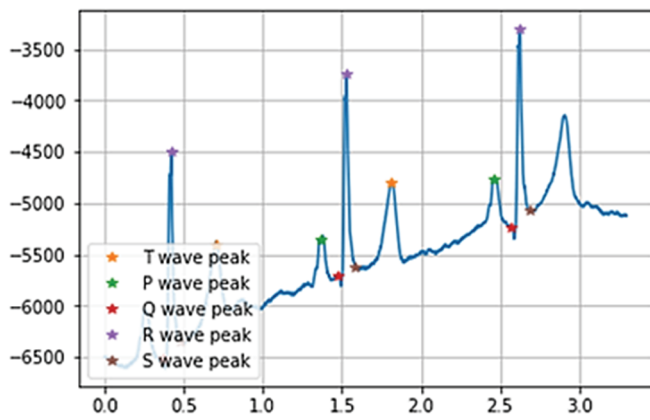


Fig. 24. Peaks classification on the original signal.

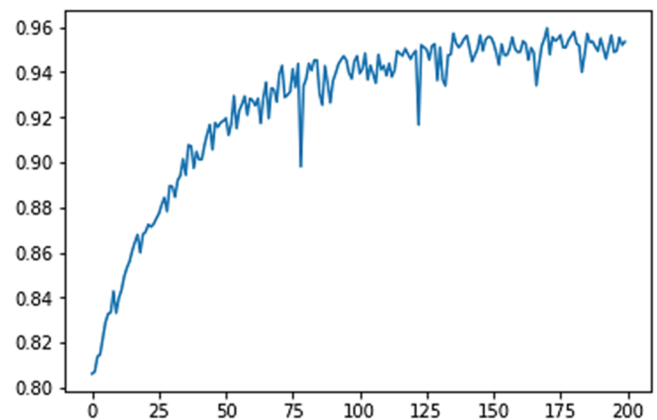


Fig. 26. Accuracy after each epoch for the CNN model.

B. Arrhythmia detection by deep learning

CNN model was trained during 200 epochs as shown in Figure 26. It was trained on a computer with intel I5-7200 2.50Gz processor for a total duration of 43 minutes.

After the training, the model obtains an average of 92.1% for the accuracy, 91.8% for the sensitivity and a specificity of 94.5%. The detailed results are presented in Table III.

TABLE III
RESULTS FOR CNN MODEL (SVEB: SUPRAVENTRICULAR ECTOPIC BEAT, VEB: VENTRICULAR ECTOPIC BEAT, F: FUSION BEAT, Q: UNKNOWN BEAT)

| Name | Number of records | Accuracy % | Sensitivity % | Specificity % |
|------|-------------------|------------|---------------|---------------|
| N | 2000 | 93.7 | 94.6 | 94.5 |
| SVEB | 2000 | 94.8 | 98.3 | 89.3 |
| VEB | 2000 | 91.5 | 91.4 | 92.8 |
| F | 774 | 92.2 | 86.0 | 96.8 |
| Q | 2000 | 88.2 | 88.7 | 99.2 |

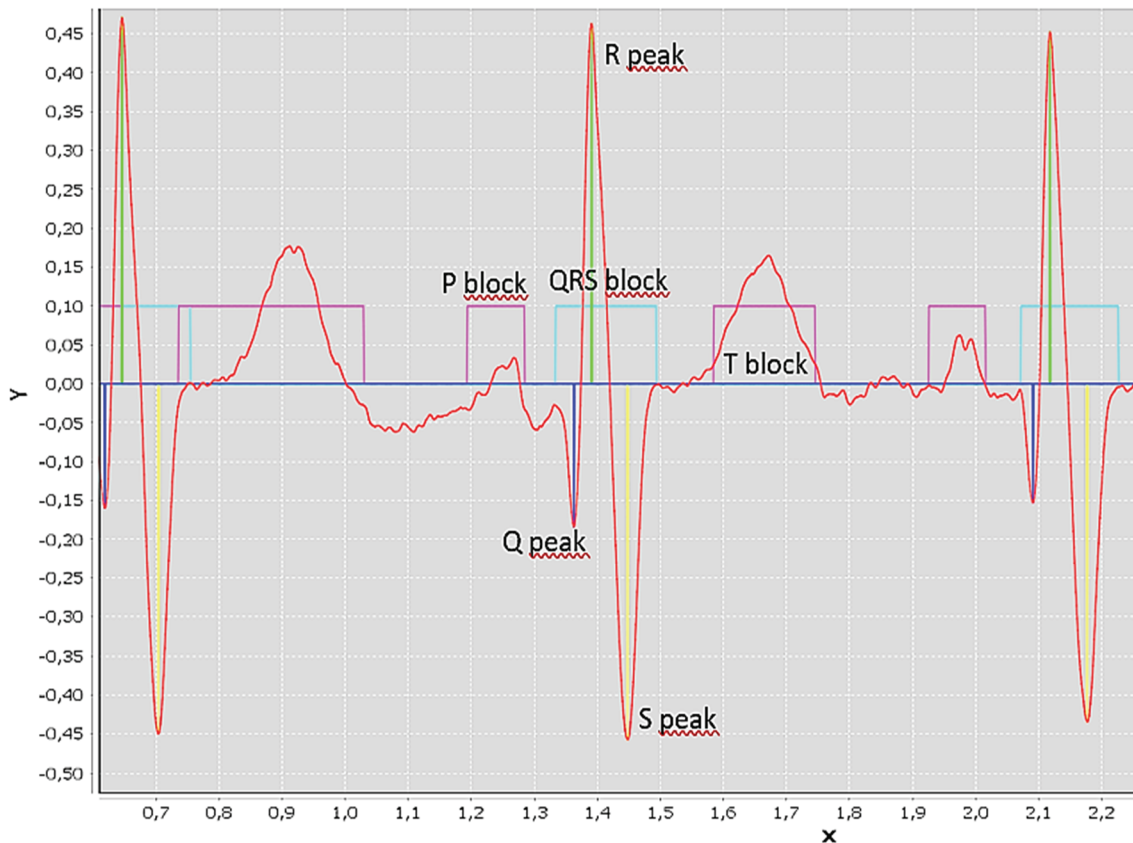


Fig. 25. Final detection signal of the patient 001.

LSTM model was trained during 45 epochs as shown in Figure 27. It took about 2 hours and 40 minutes.

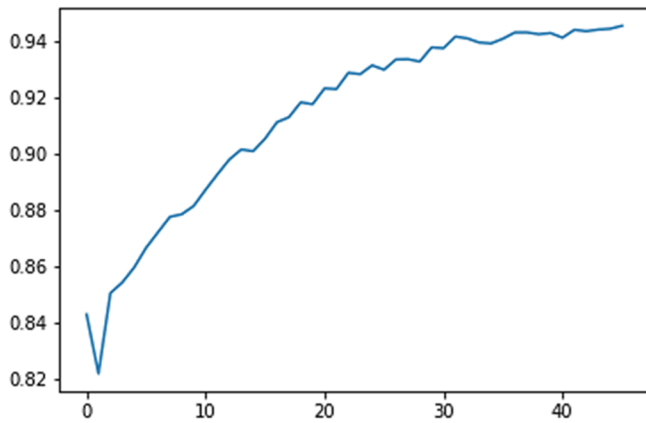


Fig. 27. Accuracy after each epoch for the LSTM Model.

The LSTM model obtains a slightly better performance, with an average of 93.6% for the accuracy, 93.1% for the sensitivity and 93.7% for the specificity. The detailed results are presented in Table IV.

TABLE IV
RESULTS FOR LSTM MODEL (SVEB: SUPRAVENTRICULAR ECTOPIC BEAT, VEB: VENTRICULAR ECTOPIC BEAT, F: FUSION BEAT, Q: UNKNOWN BEAT)

| Name | Number of records | Accuracy % | Sensitivity % | Specificity % |
|------|-------------------|------------|---------------|---------------|
| N | 2000 | 97.6 | 97.1 | 98.5 |
| SVEB | 2000 | 93.7 | 97.2 | 86.6 |
| VEB | 2000 | 92.2 | 88.6 | 97.4 |
| F | 774 | 88.3 | 87.1 | 88.7 |
| Q | 2000 | 96.3 | 95.5 | 97.3 |

IV. DISCUSSION

A. P-QRS-T waves detection

Detection method presented in this study is efficient but has some disadvantages:

- Bad detection caused by noise in the signal. Moreover, another filter cannot be applied as it could provoke an information loss.
- The database consists of 12-lead ECG recordings for each examination. Nevertheless, some of those signals are not used by the algorithm. Most of the cases, the detection is applied to the i or ii signal.
- All the signals of the examination can be unexploitable because of acquisition problem. That is why the software was not able to detect any information with 3% of the patients.

Implemented algorithm is based on the Pan-Tompkins algorithm. Correct detection is based on the promise that the R signal have the most important dynamic. If this promise is not respected, QRS complex, P and T waves cannot be detected.

B. Arrhythmia detection by deep learning

The results obtained with the use of machine learning techniques are very promising. However, further tests on bigger database should be performed. Moreover, the results shows that there is no need to use complex neural network to achieve significantly better results.

V. CONCLUSION

Developed software during this study allows for ECG signal segmentation, parameters calculation and also arrhythmias detection. It is planned to design and develop a graphic interface to present ECG signals, P-QRS-T waves and ECG parameters. Moreover, it will allow to run arrhythmias analysis and view the results of beats classification.

REFERENCES

- [1] Mendis S, Puska P, Norrving, (Eds.) B, Global Atlas on Cardiovascular Disease Prevention and Control, WHO, Geneva, 2011
- [2] Goldberger AL, Amaral LAN, Glass L, Hausdorff JM, Ivanov PCh, Ivanov PCh, Mark RG, Mietus JE, Moody GB, Peng C-K, Stanley HE. PhysioBank, PhysioToolkit and PhysioNet: Components of a New Research Resource for Complex Physiologic Signals. *Circulation* 101(23): e215-e220
- [3] Pan J, Tompkins WJ, A real-time QRS detection algorithm, IEEE TRANSACTIONS ON BIOMEDICAL ENGINEERING, VOL. BME-32, NO. 3, MARCH 1985
- [4] Buendía-Fuentes F, Arnau-Vives MA, Arnau-Vives A, et al. High-Bandpass Filters in Electrocardiography: Source of Error in the Interpretation of the ST Segment. *ISRN Cardiol.* 2012;2012:706217.
- [5] Elgendi M, Eskofier B, Abbott D (2015) Fast T Wave Detection Calibrated by Clinical Knowledge with Annotation of P and T Waves. *Sensors* 15(7): 17693-17714
- [6] Sun Y-X, Gao J, Jiang C-Y, Xue Y-M, Xu Y-Z, Liu G, Guo J-H, Sheng X, Ye Y, He H, Zhao Y-T, Barajas-Martinez H, Fu G-S and Hu D (2017) T Wave Safety Margin during the Process of ICD Implantation As a Novel Predictor of T Wave Oversensing. *Front. Physiol.* 8:659. doi: 10.3389/fphys.2017.00659
- [7] Elgendi M, Eskofier B, Abbott D. Fast T Wave Detection Calibrated by Clinical Knowledge with Annotation of P and T Waves. *Sensors (Basel)*. 2015;15(7):17693-714. Published 2015 Jul 21. doi:10.3390/s150717693
- [8] Kotas Rafał, Kamiński Marek, Mazur Piotr, Chłapiński Jakub, Sakowicz Bartosz, Napieralski Andrzej, Kurpesa Małgorzata: Project of open-source software platform for sudden cardiac death (SCD) risk stratification and advanced ECG analysis. *Przegląd Elektrotechniczny*, 2013, rocznik 89, nr 2A, s. 64-67
- [9] Bauer, A., Kantelhardt, J.W., Barthel, P., Schneider, R., Mäkikallio, T.H., Ulm, K., Hnatkova, K., Schoemig, A., Huikuri, H., Bunde, A., Malik, M., & Schmidt, G. (2006). Deceleration capacity of heart rate as a predictor of mortality after myocardial infarction: cohort study. *The Lancet*, 367, 1674-1681.
- [10] <https://physionet.org/physiobank/database/mitdb/> (MIT-BIH database)
- [11] <https://www.physionet.org/pn3/incartdb/> (Incart database)



Louis Delarue, is a student at ISEN Lille (Institute of Electronics and Digital Engineering, France). His experience is related to software development in the field of cybersecurity and artificial intelligence.



Jean Joulia is a student at ISEN Lille (Institute of Electronics and Digital Engineering, France). His experience is related to software development in the field of web applications development, audio signal processing and Arduino projects.



Pierre-Arnaud Drouard is a student at ISEN Lille (Institute of Electronics and Digital Engineering, France). His experience is related to software development in the field of signal processing and artificial intelligence.



Victorien Renault is a student at ISEN Lille (Institute of Electronics and Digital Engineering, France). His experience is related to software development in the field of signal processing and Arduino projects.



Pierre Hourdé is a student ISEN Lille (Institute of Electronics and Digital Engineering, France). His experience is related to software development in the field of mobile applications development and artificial intelligence.



Rafal Kotas received the M.Sc. and Ph.D. degrees from the Lodz University of Technology in 2009 and 2014 respectively. Since November 2014 until now he is with the Department of Microelectronics and Computer Science, Lodz University of Technology. His main field of study is processing and analysis of bioelectric signals for the purpose of medical diagnosis, web and mobile applications development, industrial electronics systems, PLC programming, SCADA and MES systems.